IOSR Journal of Mechanical and Civil Engineering (IOSR-JMCE)
e-ISSN: 2278-1684,p-ISSN: 2320-334X, Volume 19, Issue 3 Ser. IV (May. – June. 2022), PP 19-27
www.iosrjournals.org

Stability Analysis of Thin CSCS and CSSS Isotropic Plates Subjected to Vibrational Loads

Nwachukwu, U.C.[1], Opara, H.E.[2], Ihemegbulem, E.O.[3], and Oyathelemi, E.O.[4]
[1](*Civil Engineering Technology Department, Auchi Polytechnic, Auchi, Edo State, Nigeria)*
[2](*Civil Engineering Department, Imo State University, Owerri, Imo State, Nigeria)*
[3](*Civil Engineering Department, Federal University of Technology, Owerri, Imo State, Nigeria)*
[4](*Minerals and Petroleum Resources Engineering Technology Department, Auchi Polytechnic, Auchi, Edo State, Nigeria)*

Abstract
This paper applied Ritz method in the stability analysis of thin CSCS and CSSS isotropic plates subjected to vibrational load. From principles of theory of elasticity, the total potential energy functional for a thin plate was derived. By minimization method, the total potential functional was differentiated with respect to deflection coefficient through which a unique governing equation for critical buckling load subjected to vibrational load was obtained. The shape functions used in this study are of polynomial family. Applications of the derived equation for thin CSCS and CCCS plates were performed. Comparing the results of non – dimensional critical buckling load of the earlier and present studies for thin CSCS and CSSS plates at aspect ratios $(1.0 \leq P \leq 2.0)$*, it was noticed that their maximum absolute percentage differences (%) are 0.195 and 0.006 respectively. This shows that very close values were given by the earlier studies and this study. In addition, the non – dimensional critical buckling loads for CSCC and CSSS plates subjected to vibrational load* $(0 \leq n \leq 1.0)$ *at corresponding aspect ratios* $(1.0 \leq P[\leq 2.0)$ *were determined.*

Keywords*: Ritz Method, Total potential energy functional, Strain energy, Buckling load, Vibrational load*

List of notations
m = Mass of the structural plate
E = Modulus of elasticity of structural plate
h = Thickness of the structural plate
μ = Poisson's ratio of the structural plate
a = Structural plate length in x – axis
b = Structural plate length in y – axis
S = Simply supported edge
C = Clamped edge
F = Free edge
D = Flexural rigidity of Structural plate

Date of Submission: 01-06-2022 Date of Acceptance: 13-06-2022

I. Introduction

Plate is a solid that consist of two parallel surfaces separated by a small dimension which is its thickness. They are extensively used in architectural structures, hydraulic structures, pavements, containers, airplanes, missiles, ship hulls, offshore platform etc. The analysis of stability problems of plate carrying in plane compressive loads is important in structures due to the relatively poor capacity of plates in resisting compressive forces [1,2,4,7,14,15,18]. It is also important due to the non – linear, sudden nature of buckling. A good knowledge of buckling loads and the associated buckling mode shapes is fundamental to structural analysis and design for compressed plates; hence the need for the development of effective methods such as numerical and analytical approaches for solving the buckling problems. Many research works have been carried out in buckling, bending and free vibration of plates. Timoshenko [14, 15] obtained solutions on the governing domain differential equation for the elastic buckling of thin rectangular isotropic homogeneous plates subjected to uniaxial uniform compressive load for different types of boundary conditions. He applied the Navier's double trigonometric series method and the total potential energy minimization method to obtain the characteristic buckling equations, which he solved to determine the buckling loads. Onyia et al. [13] worked on the elastic

buckling analysis of SSCF and SSSS rectangular thin plate using single finite Fourier sine integral transform method. They obtained the governing equation for solving elastic buckling loads for both SSCF and SSSS plates. Uzoukwu et al. [16] worked on the stability analysis of rectangular CCSS and CCCS isotropic plates using 3rd order energy functional. They obtained the general critical buckling load equation used in solving the non – dimensional buckling loads for both CCSS and CCCS plates. Onwuka et al. [11] worked on the buckling analysis of biaxially compressed all round simply supported (SSSS) thin rectangular isotropic plate using Galerkin's method. They formulated critical buckling load equation for solving the buckling loads for SSSS plate. Iyengar [7] applied Galerkin's method in analysis of the elastic buckling of SSSS plate subjected to uniform uniaxial loads. He obtained the plate's critical load by assuming the deflection function of the plate in the form of truncated double Fourier series. Kermanshahi and Neyestanak [8] worked on exact vibration and bucking solution of Levy type initially stressed rectangular thin plates. They obtained the buckling loads and frequency parameters for SCSC, SSSC, SSSS, SCSF, SSSF and SFSF plates. Onyeka et al. [12] developed a new trigonometric shear deformation plate theory for the buckling analysis of a three dimensional thick CSSS rectangular isotropic plate under uniaxial compressive load using the Variational Energy approach. Onah et al. [10] worked on the elastic buckling analysis of uniaxially compressed CCSS Kirchhoff plate using single finite Fourier sine integral transform method. Okafor and Udeh [9] worked on the direct method of analysis of an isotropic rectangular plate using characteristics orthogonal polynomials. They obtained various polynomial shape functions and determined the critical non – dimensional buckling loads of plates such as SSSS, CCCC, CSSS, CCSC, CSCS and CCSS plates. Ezeh et al. [3] used polynomial shape function in the buckling analysis of CCFC rectangular plate. Recently, some researchers have used polynomial - trigonometric shape function to obtain solutions on the buckling of CSCS as well as CSSS plates subjected to vibrational loads using Split – deflection method but none has considered them using Ritz method. Thus, this paper applied polynomial shape functions to solve the buckling problems of CSCS and CSSS plates subjected to vibrational loads using Ritz Method. Typical examples of CSCS and CSSS plates subjected to both in – plane and vibrational loads are shown in Figure 1 and Figure 2 respectively.

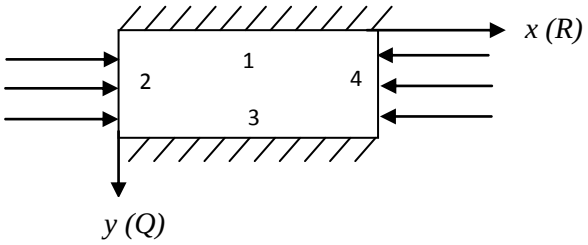

Figure 1: CSCS plate subjected to in-plane and vibrational loads

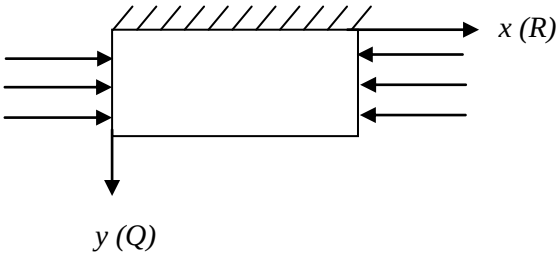

Figure 2: CSSS plate subjected to in-plane and vibrational loads

Ibearugbulem et al. [5] gave the boundary conditions for CSCS and CSCS plates at $x-$axis as;

CSCS: $w=(R=0)=\frac{d^2w_{(R=0)}}{dR}=0$; $w=(R=1)=\frac{d^2w_{(R=1)}}{dR^2}=0$

CSSS: $w=(R=0)=\frac{d^2w_{(R=0)}}{dR^2}=0$; $w=(R=1)=\frac{d^2w_{(R=1)}}{dR^2}=0$

II. Materials and Methods

The materials used in this study are already existing equations that are of common knowledge.

According to Ventsel and Krauthammer (2001), Kirchhoff in 1850 gave the following kinematic assumptions on thin plates as;

- the displacements at x and y directions respectively are given in Equations (1) and (2) as:

$$u=-Z\frac{dw}{dx} \quad (1)$$

$$v=-Z\frac{dw}{dy} \quad (2)$$

- the strain – displacement relations for thin plates are given in Equations (3), (4) and (5) as:

$$\varepsilon_x=\frac{du}{dx}=-Z\frac{d^2w}{dx^2} \quad (3)$$

$$\varepsilon_y = \frac{dv}{dy} = -Z\frac{d^2w}{dy^2} \quad (4)$$

$$Y_{xy} = \frac{du}{dy} + \frac{dv}{dx} = -2Z\frac{d^2w}{dxdy} \quad (5)$$

- the stress – strain relations for thin plates are given in Equations (6), (7) and (8) as:

$$\sigma_x = \frac{E}{1-\mu^2}[\varepsilon_x + \mu\varepsilon_y] \quad (6)$$

$$\sigma_y = \frac{E}{1-\mu^2}[\mu\varepsilon_x + \varepsilon_y] \quad (7)$$

$$\tau_{xy} = \frac{E(1-\mu)}{2(1-\mu^2)}\gamma_{xy} \quad (8)$$

The methods involved in this research work are given as follows;

Stress – Displacement Relations

Substituting Equations (3), (4) and (5) into Equations (6), (7) and (8) give Equations (9), (10) and (11) as:

$$\sigma_x = -\frac{EZ}{1-\mu^2}[\frac{d^2w}{dx^2} + \mu\frac{d^2w}{dy^2}] \quad (9)$$

$$\sigma_y = -\frac{EZ}{1-\mu^2}[\mu\frac{d^2w}{dx^2} + \frac{d^2w}{dy^2}] \quad (10)$$

$$\tau_{xy} = -\frac{EZ(1-\mu)}{(1-\mu^2)}\frac{\mathrm{d^2w}}{dxdy} \quad (11)$$

Strain Energy Equation

The strain energy is given as:

$$\mathrm{U} = \frac{1}{2}\int_0^a \int_0^b [\int_{-\frac{t}{2}}^{\frac{t}{2}} (\sigma_x\varepsilon_x + \sigma_y\varepsilon_y + \tau_{xx}\gamma_{xy})\mathrm{dz}]\mathrm{dxdy} \quad (12)$$

Substituting Equations (6), (7), (8), (9), (10) and (11) into Equation (12) gives strain energy as:

$$U = \frac{D}{2}\int_0^a \int_0^b [(\frac{d^2w}{dx^2})^2 + 2(\frac{d^2w}{dxdy})^2 + \left(\frac{d^2w}{dy^2}\right)^2]dxdy$$

That is;

$$U = \frac{D}{2}[\int_0^a \int_0^b (\frac{d^2w}{dx^2})^2 dxdy + \frac{2D}{2}[\int_0^a \int_0^b \left(\frac{d^2w}{dxdy}\right)^2 \mathrm{dxdy}] + \frac{\mathrm{D}}{2}[\int_0^a \int_0^b (\frac{d^2w}{dy^2})^2 dxdy] \quad (13)$$

Where; $D = \frac{Eh^3}{12(1-\mu^2)}$

External Work Equation

The external work done by the in-plane compressive load is given as:

$$V_1 = \frac{N_x}{2}\int_0^a \int_0^b (\frac{dw}{dx})^2\, dxdy \quad (14)$$

The external work done by the vibrational load is given as:

$$V_2 = \frac{m\lambda^2}{2}\int_0^a \int_0^b w^2\, dxdy \quad (15)$$

The total external work is obtained by adding Equation (14) and Equation (15) as:

$$V = \frac{N_x}{2}\int_0^a \int_0^b (\frac{dw}{dx})^2\, dxdy + \frac{m\lambda^2}{2}\int_0^a \int_0^b w^2\, dxdy \quad (16)$$

Total Potential Energy Equation

Equation (13) minus Equation (16) gives the total potential energy functional, Π as:

$$\Pi = \frac{D}{2}[\int_0^a \int_0^b (\frac{d^2w}{dx^2})^2 dxdy] + \frac{2D}{2}[\int_0^a \int_0^b \left(\frac{d^2w}{dxdy}\right)^2 \mathrm{dxdy}] + \frac{\mathrm{D}}{2}[\int_0^a \int_0^b (\frac{d^2w}{dy^2})^2 dxdy] -$$
$$\frac{1}{2}[N_x \int_0^a \int_0^b \left(\frac{dw}{dx}\right)^2 + m\lambda^2 \int_0^a \int_0^b w^2]\, dxdy \quad (17)$$

Let the deflection function, w be given as:

$$w = AH \tag{18}$$

Where A represents the deflection coefficient and H is the shape function.

Substituting Equation (18) into Equation (17) gives:

$$\Pi = \frac{\mathrm{A^2D}}{2}\left[\int_0^a \int_0^b \left(\frac{d^2H}{dx^2}\right)^2 dxdy\right] + \frac{2\mathrm{A^2D}}{2}\left[\int_0^a \int_0^b \left(\frac{d^2H}{dxdy}\right)^2 \mathrm{dxdy}\right] + \frac{\mathrm{A^2D}}{2}\left[\int_0^a \int_0^b \left(\frac{d^2H}{dy^2}\right)^2 dxdy\right] - \frac{\mathrm{A^2}}{2}\left[N_x \int_0^a \int_0^b \left(\frac{dH}{dx}\right)^2 + m\lambda^2 \int_0^a \int_0^b H^2\right] dxdy \tag{19}$$

Equation (19) can be written in non – dimensional R and Q axes given in Equations (20) and (21) as:

$$x = aR \tag{20}$$

$$y = bQ \tag{21}$$

Let the aspect ratio, $P = \frac{b}{a}$ (22)

Substituting Equations (20), (21) and (22) into Equation (19) gives:

$$\Pi = \frac{\mathrm{abA^2D}}{2\mathrm{a}^4}\left[\int_0^1 \int_0^1 \left(\frac{d^2H}{dR^2}\right)^2 dRdQ\right] + \frac{2ab\mathrm{A^2D}}{2a^4P^2}\left[\int_0^1 \int_0^1 \left(\frac{d^2H}{dRdQ}\right)^2 \mathrm{dRdQ}\right] + \frac{\mathrm{abA^2D}}{2a^4P^4}\left[\int_0^1 \int_0^1 \left(\frac{d^2H}{dQ^2}\right)^2 dRdQ\right] - \frac{\mathrm{abA^2}}{2a^2}\left[N_x \int_0^1 \int_0^1 \left(\frac{dH}{dR}\right)^2 dRdQ + m\lambda^2 \int_0^1 \int_0^1 H^2\, dRdQ\right] \tag{23}$$

Minimization of Total Potential Energy Functional

Differentiating Equation (23) with respect to the deflection coefficient, A gives:

$$\frac{d\,\Pi}{dA} = \frac{\mathrm{AD}}{\mathrm{a}^4}\left[\int_0^1 \int_0^1 \left(\frac{d^2H}{dR^2}\right)^2 dRdQ\right] + \frac{2\mathrm{AD}}{a^4P^2}\left[\int_0^1 \int_0^1 \left(\frac{d^2H}{dRdQ}\right)^2 \mathrm{dRdQ}\right] + \frac{\mathrm{AD}}{a^4P^4}\left[\int_0^1 \int_0^1 \left(\frac{d^2H}{dQ^2}\right)^2 \mathrm{dRdQ}\right] - \frac{\mathrm{A}}{a^2}\left[N_x \int_0^1 \int_0^1 \left(\frac{dH}{dR}\right)^2 dRdQ + m\lambda^2 \int_0^1 \int_0^1 H^2\, dRdQ\right] = 0$$

That is;

$$\frac{\mathrm{D}}{\mathrm{a}^2}\left[\int_0^1 \int_0^1 \left(\frac{d^2H}{dR^2}\right)^2 dRdQ\right] + \frac{2\mathrm{D}}{a^2P^2}\left[\int_0^1 \int_0^1 \left(\frac{d^2H}{dRdQ}\right)^2 \mathrm{dRdQ}\right] + \frac{\mathrm{D}}{a^2P^4}\left[\int_0^1 \int_0^1 \left(\frac{d^2H}{dQ^2}\right)^2 \mathrm{dRdQ}\right] = \left[N_x \int_0^1 \int_0^1 \left(\frac{dH}{dR}\right)^2 dRdQ + m\lambda^2 \int_0^1 \int_0^1 H^2\, dRdQ\right] \tag{24}$$

Re-arranging Equation (24) gives:

$$\frac{D}{a^2}\left[K_x + \frac{2}{P^2}K_{xy} + \frac{1}{P^4}K_y\right] = \left[N_x K_{Nx} + m\lambda^2 K_\lambda\right] \tag{25}$$

Where the stiffness coefficients are given in Equations (26), (27), (28), (29) and (30) as:

$$K_x = \int_0^1 \int_0^1 \left(\frac{d^2H}{dR^2}\right)^2 dRdQ \tag{26}$$

$$K_{xy} = \int_0^1 \int_0^1 \left(\frac{d^2H}{dRdQ}\right)^2 \mathrm{dRdQ} \tag{27}$$

$$K_y = \int_0^1 \int_0^1 \left(\frac{d^2H}{dQ^2}\right)^2 \mathrm{dRdQ} \tag{28}$$

$$K_{Nx} = \int_0^1 \int_0^1 \left(\frac{dH}{dR}\right)^2 dRdQ \tag{29}$$

$$K_\lambda = \int_0^1 \int_0^1 H^2\, dRdQ \tag{30}$$

Under vibration only, Equation (25) becomes:

$$\frac{D}{a^2}\left[K_x + \frac{2}{P^2}K_{xy} + \frac{1}{P^4}K_y\right] = m\lambda^2 K_\lambda \tag{31}$$

Using Equation (25), the buckling load, N_x is given as:

$$N_x = \frac{\frac{D}{a^2}\left[K_x + \frac{2}{P^2}K_{xy} + \frac{1}{P^4}K_y\right] - m\theta^2 K_\lambda}{K_{Nx}} \tag{32}$$

Where θ represents the oscillatory frequency ($0 \leq \theta \leq \boldsymbol{\lambda}$), $\boldsymbol{\lambda}$ is the vibrational frequency. Substituting Equation (31) into Equation (32) we have:

$$N_x = \frac{m\lambda^2 K_\lambda - m\theta^2 K_\lambda}{K_{Nx}} \quad (33)$$

Re-arranging Equation (33) gives:

$$N_x = \frac{m\lambda^2 K_\lambda}{K_{Nx}}\left(1 - \frac{\theta^2}{\lambda^2}\right) \quad (34)$$

Substituting Equation (31) into Equation (34) gives:

$$N_x = \frac{\frac{D}{a^2}\left[K_x + \frac{2}{P^2}K_{xy} + \frac{1}{P^4}K_y\right]}{K_{Nx}}\left(1 - \frac{\theta^2}{\lambda^2}\right) \quad (35)$$

Take the vibrational frequency ratio $(n) = \frac{\theta}{\lambda}$, dimensional constant $= \frac{D}{a^2}$, aspect ratio $(P) = \frac{b}{a}$ where ($1.0 \leq P \leq 2.0$).

Equation (35) becomes:

$$N_x = \frac{\frac{D}{a^2}\left[K_x + \frac{2}{P^2}K_{xy} + \frac{1}{P^4}K_y\right]}{K_{Nx}}(1 - n^2) \quad (36)$$

Equation (36) is a unique governing equation for determining the critical buckling load for thin plate subjected to vibrational load.

III. Application of Derived Equation

❖ CSCS PLATE

The polynomial shape function for CSCS plate is given by Ibearugbulem [5] as:

$$H = (R - 2R^3 + R^4)(Q^2 - 2Q^3 + Q^4) \quad (37)$$

The derivatives of Equation (37) with respect to R and Q are given in Equations (38), (39), (40) and (41) as:

$$\left(\frac{dH}{dR}\right)^2 = (1 - 12R^2 + 8R^2 + 36R^4 - 48R^5 + 16R^6)(Q^2 - 4Q^4 + 2Q^5 + 4Q^6 - 4Q^7 + Q^8) \quad (38)$$

$$\left(\frac{d^2H}{dR^2}\right)^2 = 144\,(R^4 - 2R^3 + R^2)(Q^4 - 4Q^5 + 6Q^6 - 4Q^7 + Q^8) \quad (39)$$

$$\left(\frac{d^2H}{dQ^2}\right)^2 = (R^2 - 4R^4 + 2R^5 + 4R^6 - 4R^7 + R^8)(4 - 48Q + 192Q^2 - 288Q^3 + 144Q^4) \quad (40)$$

$$\left(\frac{d^2H}{dRdQ}\right)^2 = (1 - 12R^2 + 8R^2 + 36R^4 - 48R^5 + 16R^6)(4Q^2 - 24Q^3 + 52Q^4 - 48Q^5 + 16Q^6) \quad (41)$$

Integrating Equations (38), (39), (40) and (41) in limits (from 0 -1) with respect to R and Q give Equations (42), (43), (44) and (45) as:

$$K_x = \int_0^1 \int_0^1 \left(\frac{\mathrm{d^2H}}{\mathrm{dR^2}}\right)^2 \mathrm{dRdQ} = 0.007619 \quad (42)$$

$$K_{xy} = \int_0^1 \int_0^1 \left(\frac{d^2H}{dRdQ}\right)^2 \mathrm{dRdQ} = 0.00925 \quad (43)$$

$$K_y = \int_0^1 \int_0^1 \left(\frac{d^2H}{dQ^2}\right)^2 dRdQ = 0.039365 \quad (44)$$

$$K_{Nx} = \int_0^1 \int_0^1 \left(\frac{dH}{dR}\right)^2 dRdQ = 0.0007709 \quad (45)$$

Substituting Equations (42) to (45) into Equation (36) gives:

$$\tilde{N}_x = \left[9.883 + \frac{23.998}{P^2} + \frac{51.06}{P^4}\right](1 - n^2) \quad (46)$$

Equation (46) is the specific equation for determining the non – dimensional buckling load for thin CSCS plate subjected to vibrational load.

❖ CSSS PLATE

The polynomial shape function for CSSS plate is given by Ibearugbulem [5] as:

$$H = (R - 2R^3 + R^4)(1.5Q^2 - 2.5Q^3 + Q^4) \quad (47)$$

The derivatives of Equation (47) with respect to R and Q are given in Equations (48), (49), (50) and (51) as:

$$\left(\frac{dH}{dR}\right)^2 = (1 - 12R^2 + 8R^2 + 36R^4 - 48R^5 + 16R^6)(2.25Q^4 - 7.5Q^5 + 9.25Q^6 - 5Q^7 + Q^8) \quad (48)$$

$$\left(\frac{d^2H}{dR^2}\right)^2 = 144\,(R^4 - 2R^3 + R^2)(2.25Q^4 - 7.5Q^5 + 9.25Q^6 - 5Q^7 + Q^8) \quad (49)$$

$$\left(\frac{d^2H}{dQ^2}\right)^2 = (R^2 - 4R^4 + 2R^5 + 4R^6 - 4R^7 + R^8)(9 - 90Q + 297Q^2 - 360Q^3 + 144Q^4) \quad (50)$$

$$\left(\frac{d^2H}{dRdQ}\right)^2 (1 - 12R^2 + 8R^2 + 36R^4 - 48R^5 + 16R^6)(9Q^2 - 45Q^3 + 80.25Q^4 - 60Q^5 + 16Q^6) \quad (51)$$

Integrating Equations (48), (49), (50) and (51) in limits (from 0 – 1) with respect to R and Q give Equations (52), (53), (54) and (55) as:

$$K_x = \int_0^1 \int_0^1 (\frac{\mathrm{d}^2\mathrm{H}}{\mathrm{dR}^2})^2 \mathrm{dRdQ} = 0.03619 \quad (52)$$

$$K_{xy} = \int_0^1 \int_0^1 (\frac{d^2H}{dRdQ})^2 \mathrm{dRdQ} = 0.04163 \quad (53)$$

$$K_y = \int_0^1 \int_0^1 (\frac{d^2H}{dQ^2})^2 dRdQ = 0.08857 \quad (54)$$

$$K_{Nx} = \int_0^1 \int_0^1 \left(\frac{dH}{dR}\right)^2 dRdQ = 0.003662 \quad (55)$$

Substituting Equations (52), (53), (54) and (55) into Equation (36) gives:

$$\tilde{N}_x = [9.882 + \frac{22.736}{P^2} + \frac{24.186}{P^4}](1 - n^2) \quad (56)$$

Equation (56) is the specific equation for determining the non – dimensional buckling load for thin CSSS plate subjected to vibrational load.

The results of this study were compared to those from the earlier studies using percentage difference tool which is given as:

Percentage (%) difference = $\frac{N_P - N_E}{N_E} x \frac{100}{1}$

Where N_P = Result of Present study

N_E = Result of Earlier study

IV. Results and Discussion

Table 1 and Table 2 shows the comparison of the non – dimensional critical buckling loads results of thin CSCS and CSSS plates between the earlier studies and this study at aspect ratios $(1.0 \leq P \leq 2.0)$ respectively.

Table 1: Non – dimensional critical buckling load for thin CSCS plate

Aspect ratio, P	[6]	Present study	% Diff. between [6] and Present Study
1.0	85.064	84.941	- 0.145
1.1	64.688	64.591	- 0.150
1.2	51.251	51.172	- 0.154
1.3	42.028	41.961	- 0.159
1.4	35.477	35.418	- 0.166
1.5	30.687	30.635	- 0.169
1.6	27.096	27.048	- 0.177
1.7	24.344	24.300	- 0.181
1.8	22.195	22.154	- 0.184
1.9	20.488	20.448	- 0.195
2.0	19.111	19.074	- 0.194

Table 2: Non – dimensional critical buckling load for thin CSSS plate

Aspect ratio, P	[5]	Present study	% Diff. between [5] and Present Study
1.0	56.807	56.804	- 0.005
1.1	45.194	45.192	- 0.004
1.2	37.337	37.335	- 0.005
1.3	31.805	31.804	- 0.003
1.4	27.780	27.779	- 0.004
1.5	24.766	24.765	- 0.004
1.6	22.455	22.454	- 0.004
1.7	20.646	20.646	- 0.000
1.8	19.204	19.204	- 0.000
1.9	18.037	18.037	- 0.000
2.0	17.079	17.078	- 0.006

The maximum absolute percentage difference (%) between the results of the solution by Ibearugbulem et al. [6] and this study for thin CSCS plate is 0.195. Also, the maximum absolute percentage difference (%) between the results of the solution by Ibearugbulem [5] and this study for thin CSSS plate is 0.006. Comparing the results, it was noticed that this study gave insignificant percentage differences with those from the earlier studies. Hence, this paper presents the non-dimensional critical buckling load results for thin CSCS and CSSS plates subjected to vibrational loads $(0 \leq n \leq 1.0)$ at aspect ratios $(1.0 \leq P \leq 2.0)$ on Table 3 / Figure 3 and Table 4 / Figure 4 respectively.

Table 3: Non - dimensional Critical Buckling Load for thin CSCS Plate subjected to Vibrational Load

	Non – dimensional critical buckling load $(\bar{N}_x)$										
	Vibrational frequency ratio (n)										
Aspect ratio (P = b/a)	0	0.1	0.2	0.3	0.4	0.5	0.6	0.7	0.8	0.9	1.0
1.0	84.941	84.092	81.544	77.296	71.351	63.706	54.362	43.320	30.579	16.139	0
1.1	64.591	63.945	62.007	58.778	54.256	48.443	41.338	32.941	23.253	12.272	0
1.2	51.172	50.661	49.125	46.567	42.985	38.379	32.750	26.098	18.422	9.723	0
1.3	41.961	41.541	40.282	38.184	35.247	31.470	26.855	21.400	15.106	7.973	0
1.4	35.418	35.064	34.002	32.231	29.751	26.564	22.668	18.063	12.751	6.729	0
1.5	30.635	30.328	29.409	27.878	25.733	22.976	19.606	15.624	11.028	5.821	0
1.6	27.048	26.778	25.966	24.614	22.721	20.286	17.311	13.795	9.737	4.139	0
1.7	24.300	24.057	23.328	22.113	20.412	18.225	15.552	12.393	8.748	4.617	0
1.8	22.154	21.932	21.267	20.160	18.609	16.615	14.178	11.298	7.975	4.209	0
1.9	20.448	20.244	19.631	18.608	17.177	15.336	13.087	10.429	7.361	3.885	0
2.0	19.074	18.883	18.311	17.357	16.022	14.305	12.207	9.727	6.866	3.624	0

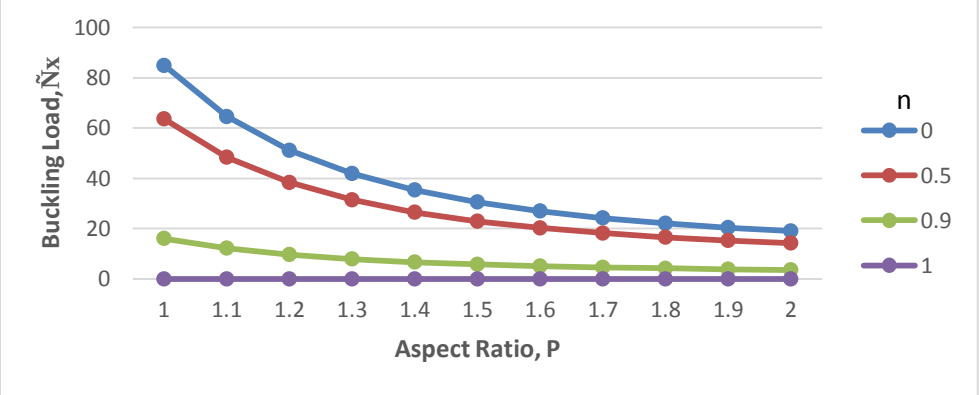

Figure 3: Non-dimensional critical buckling load for thin CSCS plate subjected to vibrational load

Table 4: Non – dimensional Critical Buckling Load for thin CSSS Plate subjected to Vibrational load

	Non – dimensional critical buckling load $(\bar{N}_x)$										
	Vibrational frequency ratio (n)										
Aspect ratio (P=b/a)	0	0.1	0.2	0.3	0.4	0.5	0.6	0.7	0.8	0.9	1.0
1.0	56.804	56.237	54.533	51.693	47.716	42.604	36.355	28.971	20.450	10.793	0
1.1	45.192	44.740	43.385	41.125	37.962	33.894	28.923	23.048	16.269	8.587	0
1.2	37.335	36.962	35.842	33.975	31.362	28.002	23.895	19.041	13.441	7.094	0
1.3	31.804	31.486	30.532	28.942	26.716	23.853	20.355	16.220	11.450	6.043	0
1.4	27.779	27.501	26.667	25.278	23.334	20.834	17.778	14.167	10.000	5.278	0
1.5	24.765	24.517	23.774	22.536	20.803	18.574	15.850	12.630	8.915	4.705	0
1.6	22.454	22.230	21.556	20.433	18.862	16.841	14.371	11.452	8.084	4.266	0
1.7	20.646	20.439	19.820	18.787	17.342	15.484	13.213	10.529	7.432	3.923	0
1.8	19.204	19.012	18.436	17.475	16.131	14.403	12.290	9.794	6.913	3.649	0
1.9	18.037	17.856	17.315	16.413	15.151	13.526	11.543	9.199	6.493	3.427	0
2.0	17.078	16.907	16.395	15.541	14.346	12.809	10.930	8.710	6.148	3.245	0

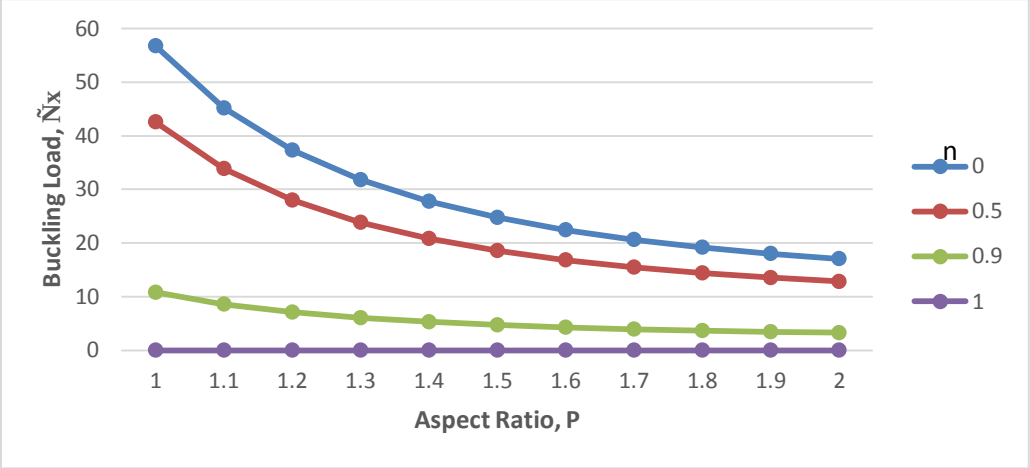

Figure 4: Non-dimensional critical buckling load for thin CSSS plate subjected to vibrational load

Table 3/Figure 3 and Table 4/Figure 4 shows that as aspect ratio ($P = \frac{b}{a}$) increases from 1.0 to 2.0 at specific vibrational frequency ratio (n), the non-dimensional critical buckling load ($\tilde{N}_x$) decreases thereby causing the plate to get more slender. Also, as the vibrational frequency ratio increases from 0 to 0.9 at specific aspect ratio, the non-dimensional critical buckling load decreases thereby causing weakening the strength of the plate and hence requires less effort to cause it to buckle. At vibrational frequency ratio($n = 1$) at all aspect ratio ($1.0 \leq P \leq 2.0$), the non-dimensional critical buckling load equals zero ($\tilde{N} = 0$). At this stage, the plate buckles without buckling load.

V. Conclusions and Recommendations

This research work presented the stability analysis of thin CSCS and CSSS plates subjected to vibrational loads. A unique governing equation for critical buckling load of plate subjected to vibrational load and the specific equations for determining the non – dimensional buckling load for thin CSCS and CSSS plates were obtained. Since the non – dimensional critical buckling load results between the earlier studies and this work specifically showed insignificant percentage differences , it follows that the results of non - dimensional critical buckling load of thin CSCS and CSSS plates subjected to vibrational load i.e at vibrational frequency ratios ($0 < n \leq 1.0$) and their corresponding aspect ratios ($1.0 \leq p \leq 2.0$) presented in Table 3/ Figure 3 and Table 4 / Figure 4 respectively for which there are no other existing results to compare with in literature are also correct. Also, for Engineering application of this research work, it is advisable to avoid vibration on plate structures irrespective of the aspect ratio because it reduces its stiffness / buckling strength. It is better to design a plate at aspect ratio, P $[\frac{b}{a}]$ = 1.0 than at P $[\frac{b}{a}] > 1.0$ because as aspect ratio increases, the stiffness strength of the plate decreases thereby making the plate to buckle faster. The equations obtained in this study are recommended for use in classical plate theory (CPT) analysis especially at aspect ratios of the form ($P = \frac{a}{b}$) to ascertain the behaviour of the plate in such conditions.

References

[1]. Bulson, P.S. (1970). The Stability of Flat Plates. Chatto and Windus, London, UK.
[2]. Chajes A. (1993). Principles of Structural Stability Theory, Englewood Cliffs New Jersey Prentice Hall.
[3]. Ezeh, J.C., Ibearugbulem, O.M., Nwadike, A.N., and Maduh, U.J. (2013). International Journal of Research in Engineering and Technology, Volume 02, Issue 12.
[4]. Gambhir, M.L. (2013). Elastic Buckling of Thin Plates in: Stability Analysis and Design of Structures, Springer Berlin Heidelberg.
[5]. Ibearugbulem, O.M. (2012). Application of a direct variational principle in Elastic Stability of Rectangular Flat Thin Plates. PhD Thesis submitted to Postgraduate School, Federal University of Technology, Owerri, Nigeria.
[6]. Ibearugbulem, O.M., Ezeh, J.C. and Ettu, L.O. (2014). Energy Methods in Theory of Rectangular Plates (Use of Polynomial Shape Functions), Liu House of Excellence Venture – Imo State, Nigeria.
[7]. Iyengar, N.G. (1988). Structural Stability of Columns and Plates. Chichester: Ellis Horwood.
[8]. Kermanshahi, M.R., and Neyestanak, A.A.L. (2013). Exact vibration and buckling solution of Levy type initially stressed rectangular thin plates. Int J Advanced Design and Manufacturing Technology,Vol. 6/ No. 4.
[9]. Okafor, F.O., and Udeh, O.T. (2015). Direct method of analysis of an isotropic rectangular plate using characteristics orthogonal polynomials. Nigerian Journal of Technolgy, Vol. 34, No. 2, pp. 232 – 239.
[10]. Onah, H. N., Nwoji, C.U., Ike, C.C., and Mama, B.O. (2018). Elastic buckling analysis of uniaxially compressed CCSS Kirchhoff plate using single finite Fourier sine integral transform method. International Information and Engineering Technology Association, Vol. 87, No. 2, pp. 107 – 111.

[11]. Onwuka, D.O., Ibearugbulem, O.M., Iwuoha, S.E.,Arimanwa, J.I., and Sule, S. (2016). Buckling Analysis of Biaxially Compressed All – Round Simply Supported (SSSS) Thin Rectangular Isotropic Plates using the Galerkin's Method. Journal of Civil Engineering and Urbanism, Volume 6, Issue 3, pp 48 – 53.
[12]. Onyeka, F.C., Okafor, F.O., and Onah, H.N. (2021). Application of a new trigonometric theory in the buckling analysis of three – dimensional thick plate. International Journal on Emerging Technologies, 12(1):228 – 240.
[13]. Onyia, M.E., Rowland-Lato, E.O., and Ike, C.C. (2020). Elastic Buckling Analysis of SSCF and SSSS Rectangular Thin Plates using the Single Finite Fourier Sine Integral Transform Method. International Journal of Engineering Research and Technology, Volume 13, Number 6, pp. 1147 – 1158.
[14]. Timoshenko, S.P., Gere, J.M. (1985). Theory of Elastic Stability. McGraw Hill, New York.
[15]. Timoshenko S. (1936). Theory of Elastic Stability, McGraw Hill Publishing Co. Ltd.
[16]. Uzoukwu, S., Ibearugbulem, O.M., Okere, C.E., and Arimanwa, J. (2021). Stability Analysis of Rectangular CCSS and CCCS Isotropic Plates using 3rd Order Energy Functional.Global Scientific Journal: Volume 9, Issue.
[17]. Ventsel, E., and Krauthammer, T. (2001). Thin Plates and Shells: Theory, Analysis and Application. New York: Marcel Dekker.
[18]. Wang, C.M., Wang, C.Y., Reddy, J.N. (2005). Exact Solution for Buckling of Structural Members. Boca Raton Florida, CRC Press LLC.

Nwachukwu, U.C, et. al. "Stability Analysis of Thin CSCS and CSSS Isotropic Plates Subjected to Vibrational Loads". *IOSR Journal of Mechanical and Civil Engineering (IOSR-JMCE),* 19(3), 2022, pp. 19-27.